Chapter 21
Flow Control Devices for Wind Turbines

Iñigo Aramendia, Unai Fernandez-Gamiz, Jose Antonio Ramos-Hernanz, Javier Sancho, Jose Manuel Lopez-Guede and Ekaitz Zulueta

Abstract The following chapter provides an overview about available knowledge, references and investigations on the active and passive flow control devices, initially developed for aeronautic industry that are currently being investigated and introduced on wind turbines. The main goal pursued with the introduction of these devices is to delay the boundary layer separation and enhance/suppress turbulences. The aim is to achieve a lift enhancement, drag reduction or flow-induced noise reduction among other parameters. However, achieving these goals present some issues, because the improvement of one of these parameters may suppose an undesired effect in another. For this reason it is necessary to study in detail each one of these devices, their operating concept, applications and their main advantages and drawbacks. Depending on the flow control nature, devices can be classified as actives or passives. Passive techniques allow to improve the performance of the

I. Aramendia (✉) · U. Fernandez-Gamiz · J. Sancho
Department of Nuclear Engineering and Fluid Mechanics,
University of the Basque Country, Nieves Cano 12,
01006 Vitoria-Gasteiz, Araba, Spain
e-mail: inigo.aramendia@ehu.eus

U. Fernandez-Gamiz
e-mail: unai.fernandez@ehu.eus

J. Sancho
e-mail: javier.sancho@ehu.eus

J.A. Ramos-Hernanz
Department of Electrical Engineering, University of the Basque Country,
Nieves Cano 12, 01006 Vitoria-Gasteiz, Araba, Spain
e-mail: josean.ramos@ehu.eus

J.M. Lopez-Guede · E. Zulueta
Department of Systems Engineering and Automatics,
University of the Basque Country, Nieves Cano 12, 01006 Vitoria-Gasteiz,
Araba, Spain
e-mail: jm.lopez@ehu.eus

E. Zulueta
e-mail: ekaitz.zulueta@ehu.eus

N. Bizon et al. (eds.), *Energy Harvesting and Energy Efficiency*,
Lecture Notes in Energy 37, DOI 10.1007/978-3-319-49875-1_21

wind turbines without external energy expenditure whereas active techniques require external energy for their activation. There are a lot of devices and in this chapter there have been compiled some of the most important ones, both passives devices (Vortex Generators, Microtabs, Spoilers, Fences, Serrated trailing edge) and actives devices (Trailing edge flaps, Air Jet Vortex Generators, Synthetic Jets).

Keywords Wind turbine · Flow control · Passive devices · Active devices · Cost of energy · Energy efficiency

Abbreviation and Acronyms

AcVG	Actuator Vortex Generator
AFC	Active Flow Control
AJVG	Air Jet Vortex Generator
CFD	Computational Fluid Dynamics
COE	Cost of Energy
DS	Delay Stall
DOF	Degree of Freedom
DTU	Danmarks Tekniske Universitet
EWEA	Energy Wind Energy Association
FEM	Finite Element Method
VG	Vortex Generator
LE	Leading Edge
MC	Mid Chord
MDO	Multidisciplinary Design Optimization
NREL	National Renewable Energy Laboratory
O&M	Operation and Maintenance
RANS	Reynolds Averaged Navier Stokes
RWT	Reference Wind Turbine
SST	Shear Stress Transport
TE	Trailing Edge
PVGJ	Pulsed Vortex Generator Jet
E_C	Kinetic Energy
ρ	Density
t	Time
C_L	Lift Coefficient
C_D	Drag Coefficient
A	Area
v	Velocity
α	Angle of Attack
c	Chord
b	Span
h	Height

21.1 Introduction

Nowadays, the depletion of global fossil fuel reserves, the environmental concerning and energy security after recent accidents as happened in Fukushima nuclear plant in Japan in 2011, has served to focus attention on the development of ecologically compatible and renewable energy sources. Besides, the power demand is also increasing more and more through new emergent economies as China, Brazil or India.

At this point, the optimization of renewable power systems (wind, solar thermal, biomass, etc.) is a key point to be able to compete in energy production and cost against the traditional energies. Wind energy becomes in a promising technology able to provide a large portion of the power requirements in many countries of the world. Wind turbines are a practical way to capture and convert the kinetic energy of the atmospheric air to either mechanic or, consequently, electrical energy.

According to EWEA [1] (European Wind Energy Association) wind power is the generating technology with the highest rate for new installations in 2014, representing the 43.7% of total power capacity, an increment of 12% in relation to 2013. Since 2000, 29.4% of new capacity installed in Europe has been wind power, 56.2% renewables and 91.1% renewables and gas combined.

The total wind power generating capacity has been increasing continuously, not only in Europe but worldwide for the last 15 years [2], as it can be seen in Fig. 21.1.

In 2015, China was the country which led the wind capacity installed, with almost a half of the total 63.000 MW, followed by the USA and Germany. 12.105 MW of the global amount capacity until 2015 corresponds to offshore installations being UK, Germany and Denmark the countries with more wind capacity installed of this type (5061, 3295 and 1271 MW respectively).

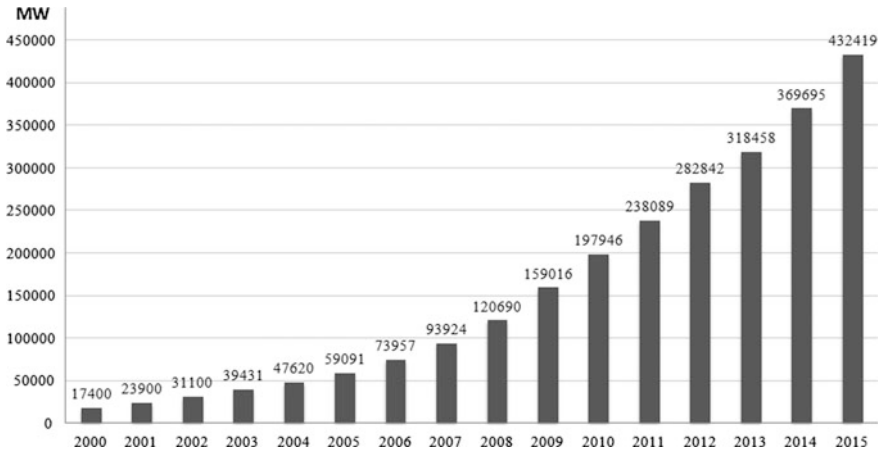

Fig. 21.1 Global cumulative installed wind capacity 2000–2015

However, even though the wind cost of energy has decreased in the last decade, a high initial investment is yet required, so it is necessary to improve its lifetime and efficiency in order to keep it economically viable.

There are several research fields to achieve this goal. Development of new materials which allow to reduce the structure weight or new blade designs just to reduce the fatigue loads and increase the aerodynamic performance of the rotors, are some of them. CFD simulations become a very interesting tool to study the behavior of this new improvements and their impact in wind turbines.

The considerable growth of wind turbines size and weight in the last years has made it impossible to control as they were controlled 30 years ago. Rotors of 120 m are now a reality. Johnson et al. [3] compiled some of the most important load control techniques that could be used in wind turbines to assure a safe and optimal operation under a variety of atmospheric conditions. They include blades made of soft, flexible materials that change shape in response to wind speed or aerodynamic loads, aerodynamically-shaped rotating towers, flexible rotor systems with hinged blades and other advanced control systems.

The higher the size of a wind turbine the higher the structural and fatigue loads. By researching and working in new and innovative load control techniques a decrease of these excessive loads could be achieved, which affect the rotor and other key components of the turbine. Loads on wind turbines are normally divided into extreme structural loads and fatigue loads. Reducing these fatigue loads is a main goal, which can reduce the maintenance costs and improve the reliability of wind turbines.

21.2 Wind Turbine Improvement Goals

The improvements of wind turbines present 3 key points [4]:

1. Setting upper bounds on and limiting the torque and power experienced by the drive train, mainly the low-speed shaft.
2. Minimize the fatigue life extraction from the rotor drive train and other structural components due to changes in wind direction, speed (including gusts), and turbulence, as well as start-stop cycles of the wind turbine.
3. Maximize the energy production.

The cost of energy (COE) [5] plays an important role inside this last key point, in order to maintain this kind of energy as a viable alternative in economic terms with traditional or other renewable energies. There are three independent variables to calculate its value as we can see in (Eq. 21.1): the total energy captured by the turbine and the costs related with the turbine (capital cost) and with the operation and maintenance (O&M) works.

$$\text{COE} = \frac{\text{Lifetime Energy Captured}}{\text{Capital Cost} + \text{O\&M Costs}} \tag{21.1}$$

The loads, directly related with the second key point, can be separated into aerodynamics and structural loads. The relative velocities around the blade sections, as a result of horizontal or vertical wind shear, turbulences and yaw and tilt misalignment, influence the aerodynamic loads on the rotor. The gravitational forces can also play a role producing periodic structural loads in the rotor blades. Control systems should be able to reduce and minimize the variation of these aerodynamic loads or to add damping to the structural nodes.

First of all, it is essential to know the relationship between the wind speed and the normalized power in a wind turbine. There are four different operating regions, as shown in Fig. 21.2, which define the power curve.

In Region 1, the wind speed is not enough to power generation. In Region 2, which lies between the cut-in velocity ($V_{cut\text{-}in}$) and rated velocity (V_{rated}), the generator works under the rated power. In Region 3, the power output is limited by the turbine. This happens when there is enough wind intensity for the turbine to reach its rated output power. The Region 4 corresponds to higher wind speed, which could shut down the turbine and even cause damage in the blades or structure of the wind turbine, with the resulting impact on maintenance costs.

The curve which separates the regions 1 and 2 shows a basic law about generation of power, where the power is directly related to the wind speed cubed. (See Fig. 21.3).

Air volume to the rotor:

$$\text{V} = \text{A} \cdot \text{v} \cdot \text{t} \tag{21.2}$$

Kinetic energy contribution from the air to the rotor:

$$E_C = \frac{1}{2} \cdot dAv \cdot t \cdot v^2 \tag{21.3}$$

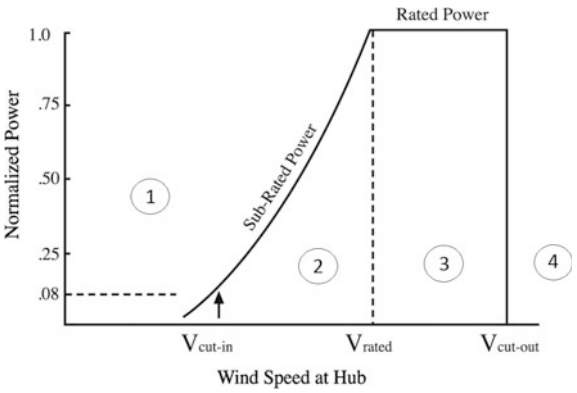

Fig. 21.2 Power curve of a wind turbine [3]

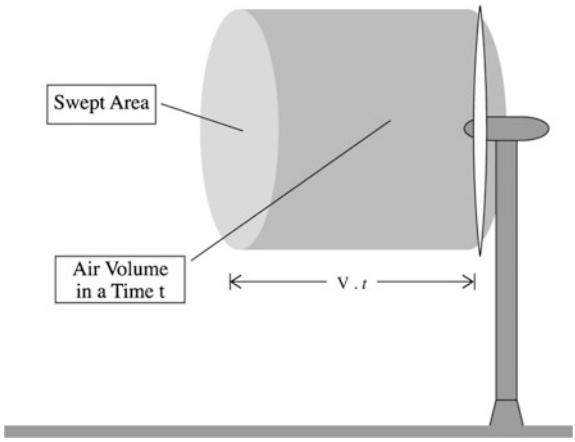

Fig. 21.3 Air volume to the rotor

Delivered power to the rotor:

$$E_C = \frac{1}{2} \cdot dA \cdot v^3 \tag{21.4}$$

21.3 Flow Control Devices Classification

Through the last decades many different flow control devices have been developed. Most of them were created for aeronautical issues and this was its first research field and application. Nowadays researchers are working to optimize and introduce this type of devices in wind turbines. Wood [6] developed a four layer scheme which allows to classify the different concepts that are part of all flow control devices (See Fig. 21.4).

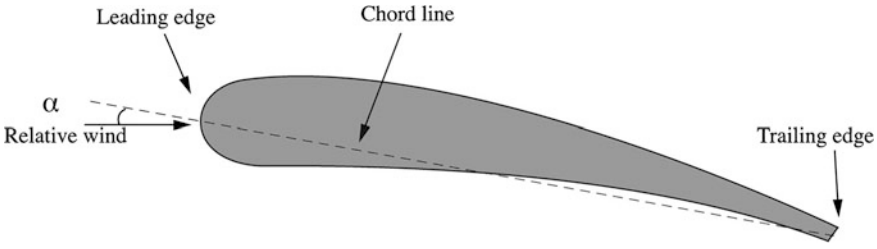

Fig. 21.4 Section and main components of an airfoil

1st Layer
According to the technique:

1. Geometric device (G): Modify the geometry and airfoil shape and thereby the airflow about it.
2. Fluidic device (F): Change the flow about the blade section by either adding air into or subtracting air from external flow.

2nd Layer
Depending on where the device is set:

1. Near the leading edge (LE).
2. Near the trailing edge (TE).
3. In the mid-chord (MC).

3rd Layer
Depending on how the device adjusts the lift curve, flow control devices modify the lift curve of an airfoil in two different ways (See Fig. 21.5).

1. Shifting the curve up (increasing lift) or down (reducing lift). (See Fig. 21.5b).
2. Extending the lift curve of the airfoil to stall at a higher angle of attack (α). (See Fig. 21.5a).

To alleviate loads successfully, it is indispensable the device to be able to reduce the generated lift. With a first watching to Fig. 21.5, it can be seen that delaying stall (DS) only increases lift at high angles of attack. For that reason devices based on DS concept would not be considered as a good alternative for load mitigation. Nevertheless, a suggestion presented by Corten [7] provides a different way of using this type of devices to mitigate turbine loads. Their main purpose is to include them to an existent profile to increase C_{Lmax} and, consequently, to delay stall. In Fig. 21.6 we can see an example with passive vortex generator (VG).

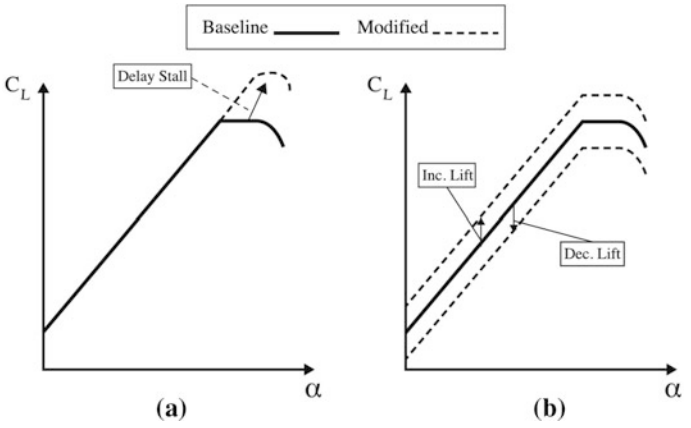

Fig. 21.5 Lift curve variation based on C_L and α [3]

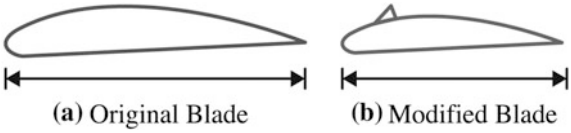

Fig. 21.6 **a** Original airfoil and **b** redesign airfoil with a VG for a same lift generation [3]

It is known that lift force is defined by the (Eq. 21.5):

$$F_L = C_{L\max} \cdot \frac{1}{2} \cdot \rho \cdot A \cdot v^2 \tag{21.5}$$

where (ρ) is air density in kg/m^3, (A) is airfoil area in m^2 and (v) is the air velocity over the blade in m/s. C_{Lmax} is the maximum lift coefficient.

The idea presented by Corten was to redesign the blade in order that the maximum sectional lift of a blade with a DS device matches that of the original blade without a DS device. Figure 21.6 illustrates the difference in chord length between both designs. Density and velocity around the blades would be equal at similar conditions. So, if C_{Lmax} is increased by the effect of the DS device, the chord (c) could be reduced an equivalent quantity according to the lift force equation, as it can be seen in (Eqs. 21.6 and 21.7).

Without a DS device

$$\mathrm{F_L} = \mathrm{C_{Lmax}} \cdot \frac{1}{2} \cdot \rho \cdot \mathrm{A} \cdot \mathrm{v}^2 = \mathrm{C_{Lmax}} \cdot \frac{1}{2} \cdot \rho \cdot (\mathrm{c} \cdot \mathrm{b}) \cdot \mathrm{v}^2 \tag{21.6}$$

With a DS device

$$F_L = C_{L\max} \uparrow \cdot \frac{1}{2} \cdot \rho \cdot A \downarrow \cdot v^2 = C_{L\max} \cdot \frac{1}{2} \cdot \rho \cdot (c \downarrow \cdot b) \cdot v^2 \tag{21.7}$$

where (c) is the chord of the blade, in meters, and (b) is the span of the blade in meters as well.

4th Layer

Depending on device working conditions, we can classify them as steady or unsteady devices (if the position of a device varies with time about a nominal setting or not). For instance, a TE flap system is considered a steady device because it changes its position to produce a sequence of steady state conditions.

21.4 Types of Devices

Depending on their operating principle they can be classified as actives or passives. This chapter is going to describe some of the main devices in each category.

(1) Passive control

(a) Vortex Generators.
(b) Microtabs.
(c) Serrated trailing edge.
(d) Fences.
(e) Spoilers.

(2) Active control

(a) Trailing-edge flaps.
(b) Synthetic jets.
(c) Air Jet Vortex Generators.

Passive control techniques represent an improvement in the turbine's efficiency and in loads reduction without external energy consumption. Active control techniques, instead, require external energy or a secondary power source. Even though, further investigations must be carried on to make sure that this raise in energy output can balance the external energy necessary for load control together with the increase in turbine capital and O&M costs.

Johnson et al. [3] made an analysis and discussed 15 different devices for wind turbine control. Some of them are still being tested on full-scale turbines.

21.4.1 Passive Control Systems

21.4.1.1 Vortex Generators

A Vortex Generator (VG) is a passive flow control device which modifies the boundary layer fluid motion bringing momentum from the outer flow region into the inner flow region of the wall bounded flow. Its main goal is to delay the flow separation and increase the maximum lift coefficient C_{Lmax}. VGs are designed to re-energize the boundary layer by inducing momentum transfer between the free stream velocity and the near wall region. The boundary layer separation begins when the portion of boundary layer closest to the wall or leading edge reverses in flow direction. (See Fig. 21.7). The separation is where the shear stress is null or close to under stall conditions.

Initially introduced by Taylor [8] VGs have been investigated for more than fifty years for a wide range of applications in aerodynamics and airplane wings. They are small vanes, usually triangular or rectangular, inclined at an angle to the incoming flow and placed as close as possible of the leading edge. They are generally assembled in a spanwise on the suction side of the blade and present the advantage that they can be added as a post-production fix to blades that do not perform as expect. Its height is usually similar to the boundary layer thickness.

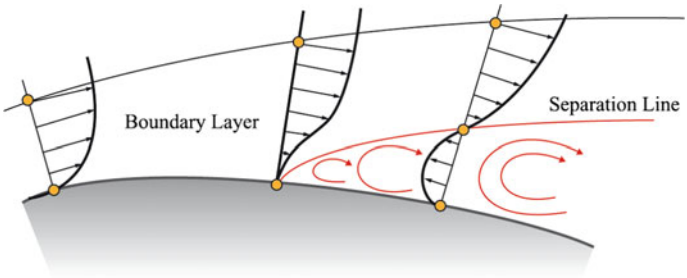

Fig. 21.7 Boundary layer separation and velocity profile with an adverse pressure gradient

Fernandez-Gamiz et al. [9] studied the behavior of a rectangular VG on a flat plane and the streamwise vortices produced by them to investigate how the physics of the wake behind VGs in a negligible streamwise pressure gradient flow can be reproduced in CFD simulations and their accuracy in comparison with experimental observations. (See Fig. 21.8).

Pearcey [10] noted that the vane type VG can be set in two basic ways, as shown in Fig. 21.9.

1. Co-rotating array: the vortices which are shed are all of the same rotational direction.
2. Counter-rotation array: the rotational sense of the vortices alternate along the array.

Godard and Stanislas [11] demonstrated that VGs work most efficiently when creating counter-rotating vortices and their geometry is triangular.

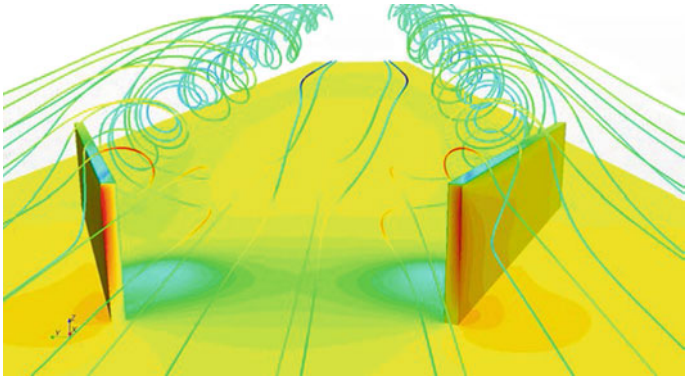

Fig. 21.8 Streamlines on a flat plane with Vortex Generators (Fernandez-Gamiz [9])

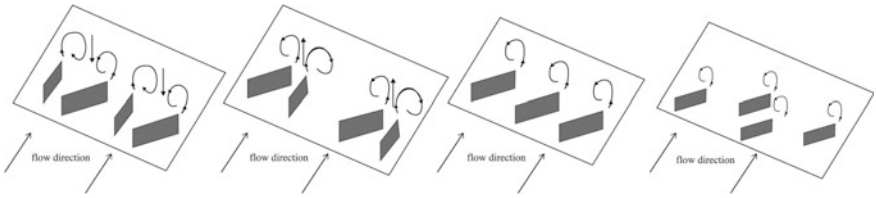

Fig. 21.9 Pairs of VGs generating co-rotating and counter-rotating vortices

In order to study the impact of VGs on wind turbines, to optimize their position and distribution, CFD tools can be used. However, modelling a fully-meshed profile with VGs becomes prohibitively expensive because of its small size (VGs height are usually equal to the boundary layer thickness). This great number of cells in the simulation becomes a trouble in computation time and therefore, in costs.

An alternative way of modeling VGs in CFD is to model the influence of the vortex generator on the boundary layer using body forces and boundary conditions generated by them. In that way, Bender et al. [12] presented the BAY model for simulating the vane vortex generators without the necessity of defining the VG geometry in the mesh. Later, Jirasek [13] introduced a new version of this model, called jBAY model, based on the lifting force theory.

Fernandez-Gamiz et al. [14] presented a detailed comparison between four different models of VGs on a flat plane. The first one is based on the traditional mesh-resolved VG. The second one, called Actuator Vortex Generator Model (AcVG), based on [12] provides an efficient method for CFD simulations of flows with VG's. The third one is an experimental model (Velte et al. [15]) based in experimental data, where measurements were carried out in a low speed closed-circuit wind tunnel. The fourth model is the analytical model of the primary vortex based on the helical structure of longitudinal embedded vortex. Following the same idea, Zamorano et al. [16] studied the evolution of the wake downstream a rectangular VG at different incidence angles. Øye [17] and Miller [18] compared, on a 1 MW wind turbine, the measured power curves with VGs and without them. Although they used quite rough methods for the VGs design optimization, both studies showed that, in these cases, VGs on average increased the output power for nearly all winds.

These devices present some important advantages, such as their small size, that allows to distribute a big number of them along the profile. They are also replaceable with no trouble in an inexpensive and uncomplicated way and they have the possibility to add them once the aerodynamic profile is built. On the other hand, their main disadvantage is the drag increases (C_D) that involve the implantation of this device, an undesirable feature for this kind of applications. Great care is also need to be taken in their blade integration not to deteriorate the performance of the wind turbine or the aeroelastic conditions.

Case Study: DTU 10 MW Reference Wind Turbine

The DTU 10 MW RWT (Reference Wind Turbine) is part of the Light Rotor Project [19]. Initiated as a cooperation of DTU Wind Energy and Vestas, its main goal is to create the design basis for next generation wind turbines of 10 MW (See Table 21.1).

The purpose of this design is [20]:

1. To achieve a design in a sequential multidisciplinary design optimization process.
2. To obtain a high-quality aerodynamic performance with lower weight.
3. To achieve a high-detail design for a complete comparison of both aero-elastic as well as high fidelity aerodynamic and structural tools.
4. To provide a openly available design basis for next generation of wind turbines.

In this project the manufacturing process is not considered, so the design does not provide a design to that end. Therefore, the purpose is not to provide a design of a complete wind turbine but of the rotor.

DTU Wind Energy developed some codes used in the design of DTU 10 MW RWT.

1. HAWC2 (Horizontal Axis Wind turbine simulation Code 2nd generation). An aeroelastic code proposed for calculating wind turbine response in time domain.
2. HAWCstab2: (Aero-servo-elastic stability tool for wind turbines).
3. BECAS. Determines cross section stiffness properties using FEM.
4. HAWTOPT (Wind turbine optimization software).
5. EllipSys2D/3D. A multiblock finite volume discretization of the incompressible of RANS equations.

Table 21.1 Key parameters of the DTU 10 MW RWT [20]

Description	Value
Rating	10 MW
Rotor orientation, configuration	Upwind, 3 blades
Control	Variable speed, collective pitch
Drive train	Medium speed, multiple stage gearbox
Rotor, hub diameter	178.3, 5.6 m
Hub height	119 m
Cut-in, rate, cut-out wind speed	4, 11.4, 25 m/s
Rated tip speed	90 m/s
Overhang, shaft tilt, pre-cone	7.07 m, 5º, 2.5º
Pre-bend	3 m
Rotor mass	229 tons (each blade ~41 tons)
Nacelle mass	446 tons
Tower mass	605 tons

ABAQUS and XFOIL were used as well for the structural design (FEM computations) and airfoil characteristics respectively.

Recently, Troldborg et al. [21] presented a case study of the DTU 10 MW RWT, making a CFD comparison with and without VGs installed on the inboard part of the blades. A personalized version of the BAY model, previously mentioned, was used in order to overcome the computational cost of simulating a blade with a large number of this type of devices on it. Forty VG pairs are distribute on each blade and were setting up in counter-rotation distribution. A grid sensitivity study was performed, with five different configurations, to check out that the model calculates the lift with precision on all grids.

The EllipSys3D flow solver was implemented which solves, in a steady state mode, the incompressible finite volume Reynolds-Averaged Navier-Stokes (RANS) equations. A fully developed turbulent boundary layer on the blade surface was assumed using the k-ω Shear SST Model [22, 23].

Figure 21.10 illustrates the rotor surface mesh, together with the VGs region as can be seen with a little more detail in the second picture, corresponding to 8 cells per VG pair and for a height of the first boundary layer of 2×10^{-6} m in order to obtain a y+ < 2.

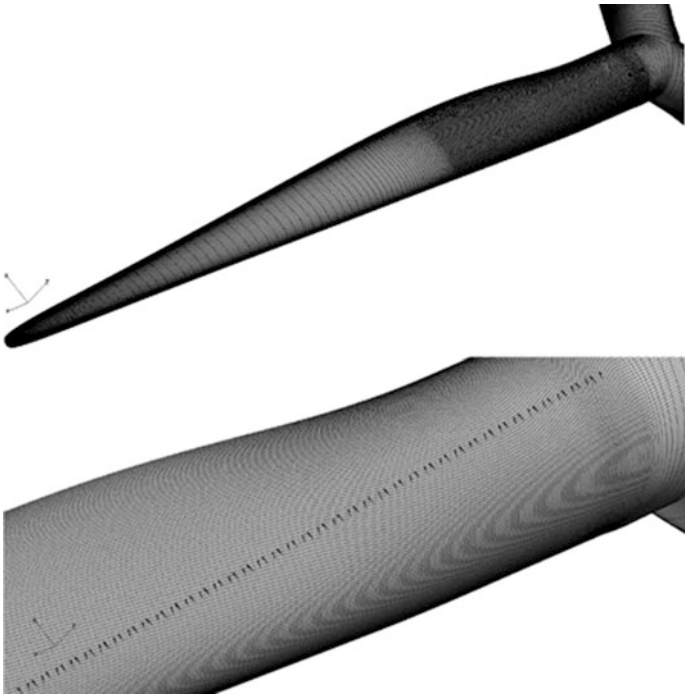

Fig. 21.10 Surface mesh for the DTU 10 MW RWT [21]

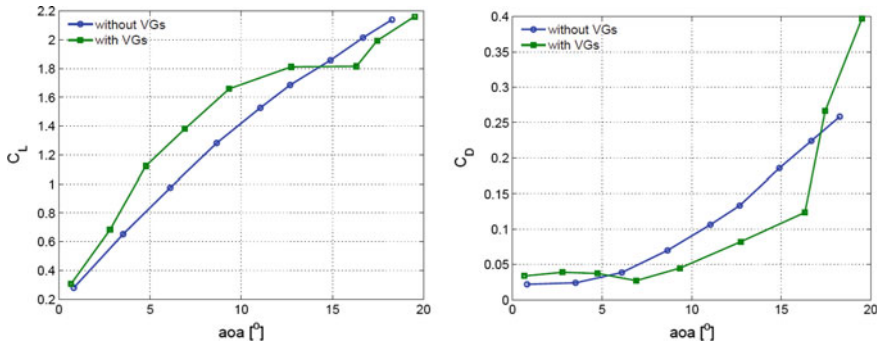

Fig. 21.11 Lift and drag polars for the section at r = 24 m (airfoil thickness 41%) [21]

The results of the simulations, in a blade with VGs, showed an increase in both tangential and normal forces at the inboard part of the blade. At the outer part of the blade, however, a slight reduction in both forces was appreciated in the case with VGs installed. The power improvement caused by the VGs is 0.51% in the best scenario studied corresponding to a wind speed of 10 m/s. Figure 21.11 shows the lift and drag curves with and without VGs at a radial position r = 24 m. It can be seen how the VGs increase the lift for a broad series of angles of attack but, on the other hand, involve a more abrupt stall which finally causes a higher drag and a lower lift.

The simulations showed a good adjustment between CFD results and wind tunnel experiments, so the 8 grid cells per VG pair can be considered enough to capture the effect of them.

21.4.1.2 Microtabs

The microtabs consist on small tabs situated near the TE of an airfoil, which projects perpendicular to the surface of the airfoil a few percent of the chord length (1–2% c) corresponding to the boundary layer thickness.

The small movement of these microtabs jets the flow in the boundary layer away from the blade's surface, bringing a recirculation zone behind the tab, as can be observed in Fig. 21.12 affects the aerodynamics shifting the point of flow separation and, therefore, providing changes in lift. Lift improvement is obtained by deploying the microtab downwards (on the pressure side) and lift reduction is obtained by deploying the microtab upwards (on the suction side).

Van Dam [25] has made multiple studies and investigations into this topic, including CFD simulations and wind-tunnel experiments in order to determine their optimal distribution height and location. The results provided, as previous studies, that the best place to situate the lower surface tab with respect to lift and drag was around 95% c with a height of 1% c and around 90% c for the upper surface tab.

They present some appealing features for wind turbine control applications:

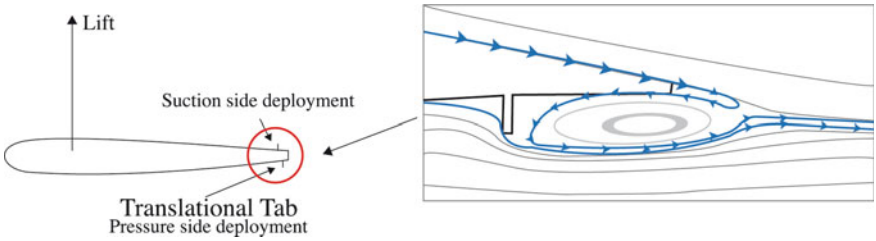

Fig. 21.12 Microtab concept and zoom of streamlines around a trailing-edge region during tab pressure side deployment (Chow and Van Dam) [24]

1. Small size.
2. Low power requirements for its activation.
3. Simplicity of the design (low cost).
4. They can be installed without significant changes in the actual techniques to manufacture the profiles.

Case Study: New Design of a Microtab Deployment Mechanism

The existing microtab device system described before presents two main drawbacks (See Fig. 21.13):

1. The insufficient tab height when it is fully-deployed.
2. The actuating mechanism which causes stiction during tab deployment.

Tsai et al. [26] presented recently and innovative design to improve the microtabs performance. The new microtab system is based on a four-bar linkage that overcomes the two disadvantages previously mentioned and providing:

1. An increase of the maximum tab height in relation to the existing microtab system. From 1 to 1.7% c.
2. A higher stability due to the four-bar linkage mechanism.

The four-bar linkage mechanism has four links and pivot joints (See Fig. 21.14); and therefore a DOF = 1. The degree of freedom (DOF) of a mechanism, i.e. the number of independent moves it has, is defined by Gruebler's equation:

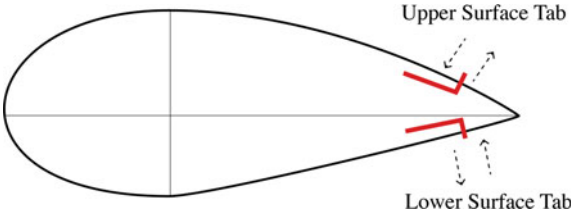

Fig. 21.13 Existing microtab actuation system [26]

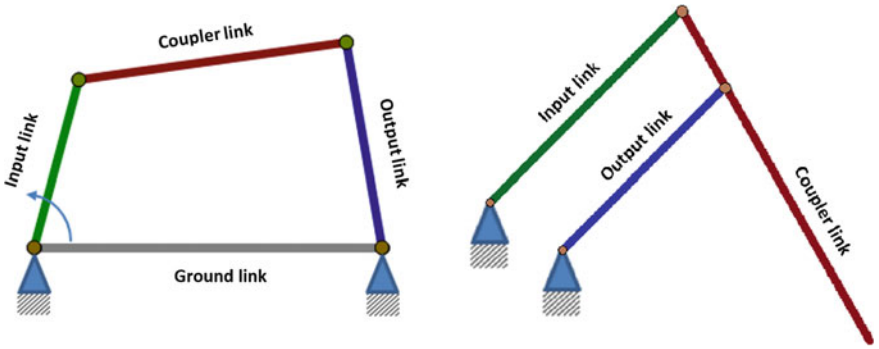

Fig. 21.14 Four-bar linkage scheme and the new scheme which is used for the microtab

$$DOF = 3(N - 1) - 2M \tag{21.8}$$

where M is the number of pivot joints and N is the number of links.

The input link is connected to an actuator which is the responsible for controlling the movement of the system, retracting or extending the microtab. Due to the space limitations in the trailing edge, the microtab cannot be positioned normal to the lower surface but a tilting angle is required. The steadiness and reliability improvement is achieved using five links (three input links and two output links) instead of the lever arm which is used in the existing microtabs.

In normal conditions, this new microtab will describes a curved trajectory throughout its deployment and retraction. To avoid that and to remain a simple straight line motion the actuator input bar is transformed into a V-shape. The measurements of the links and their angles, the stroke length and the slot length were also calculated as well as the force of the actuator.

21.4.1.3 Serrated Trailing Edge

Wind turbine noise is one of the main issues for the widespread use of wind energy. The sources of aerodynamic noise can be divided into [27]:

1. *Airfoil self-noise*: is produced by the blade in an undisturbed inflow and it is caused due to the interaction between an airfoil blade and the turbulence produced in its own boundary layer and near wake. Self-noise can be tonal or broadband in character and may be caused by several mechanisms, such as laminar boundary-layer vortex-shedding noise, turbulent boundary-layer/trailing edge interaction noise (trailing-edge noise), blade tip noise or trailing-edge bluntness noise.
2. *Inflow-turbulence noise*: it depends on the atmospheric conditions and it is caused by the interaction of upstream atmospheric turbulence with the blade.

Originally, the aerodynamic surfaces of wind turbine blades have sharp or moderately blunt trailing edges from which the wake is shed. The shedding of the wake and the confluence of flow from the pressure and suction sides of the profile are sources of aerodynamic noise, and increased drag and reduced lift. It has long been recognized that airfoil trailing edge noise may be reduced by modifying the trailing edge geometry so that the efficiency by which vorticity is scattered into sound is reduced. One alternative to resolve this trouble was patented by Siemens [28] and consists in a flexible serrated trailing edge, also known as Dino Tail, shown in Fig. 21.15.

Over the years, the characteristics and properties of airfoil noise have been studied extensively in both theoretical and experimental investigations. Both inflow turbulence and self-noise mechanisms were considered and dependence on parameters such as flow speed, angle of attack or radiation direction was studied by Howe [29]. About experimental studies, Oerlemans et al. [30] carried out different investigations where they tested the noise reduction in NACA 64418 airfoil and in blades of 2.3 MW wind turbine.

As an added aerodynamic profile, it presents the advantage of creating a customized geometry profile for each device according to the operating conditions in which it is located (See Fig. 21.16).

21.4.1.4 Fences

Fences, a system patented in 2009, consist in fin-like vertical surfaces attached to the upper surfaces of the wing that are used to control the airflow [31]. Their purpose is to disrupt the spanwise airflow, protecting the outboard wing section from a developing inboard stall. So, keeping the outboard section from stalling,

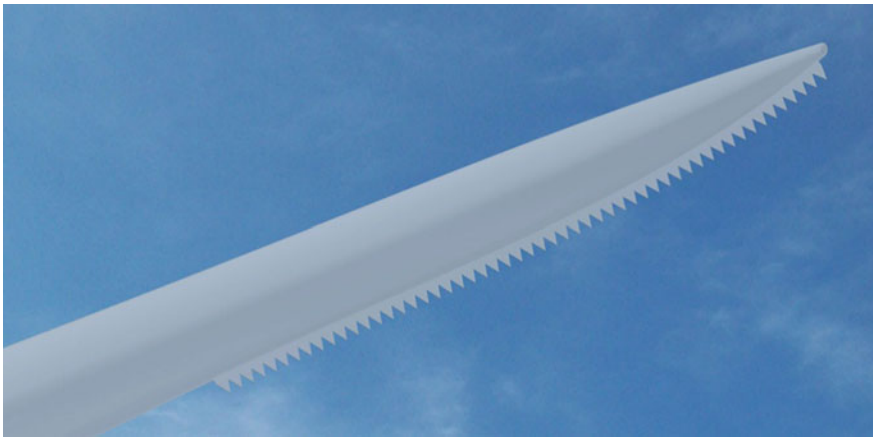

Fig. 21.15 Wind turbine blade with serrated trailing edge device

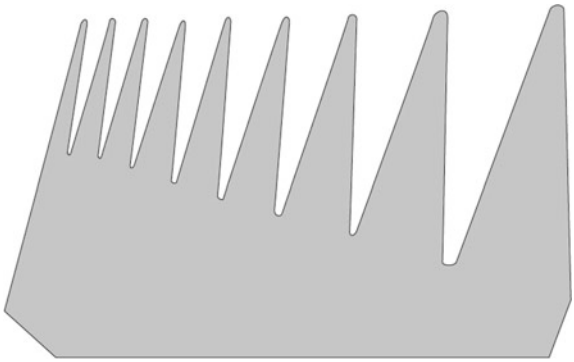

Fig. 21.16 Sawtooth trailing-edge serrations

aileron effectiveness is maintained during a stall, enabling the pilot to keep the aircraft level and exit the stall safety.

On straight wing airplanes they control the airflow in the flap area and on swept wing airplanes they prevent the accumulation of air toward the tip at high angles of attack placing them at about two-thirds of the way out towards the wing tip. In both cases, they give better slow speed handling and stall characteristics (See Fig. 21.17).

On wind turbines, the airflow also spreads in spanwise direction of the blades. This airflow generate adverse consequences in wind turbines performance, particularly because contribute to the separation of the main airflow of the blade surface, and therefore, reduce the rotor blade lift.

In order to fix that problem a fence is placed (See Fig. 21.18) extending through the entire blade surface in chord-wise direction, to prevent the creation of these airflows. This barrier or wall delay this effect by preventing the spanwise flow from moving too far along the wing and gaining speed.

The extent to which the fence is able to prevent these airflows is directly related to the fence height. However, the higher the height, the higher the weight, besides the fact that it affects to other aerodynamic characteristics of the blade, as the lift. So, it comes to choose a fence design that does not get worse the blade qualities, even though does not remove the spanwise airflow completely.

The required height and length of the particular planar element and the optimal position of this element on the suction side of the rotor blade inherently varies with the distance from the rotor axis of rotation, the blade contour depth, the rotor width, the most likely speed of the incident airflow, etc. So, the best configuration is determined empirically.

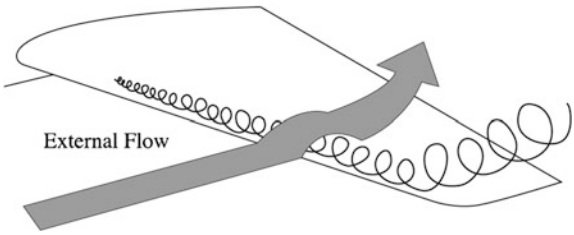

Fig. 21.17 Spanwise airflow through the blade

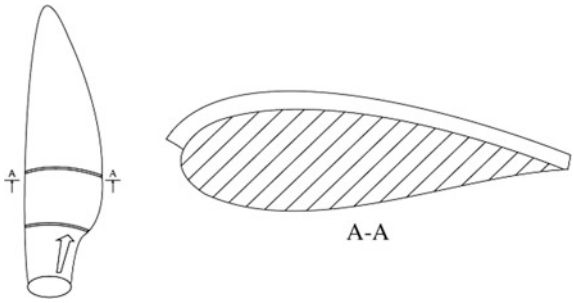

Fig. 21.18 Sketch of wind turbine blade with a fence installed and its section A-A [31]

Chow and Van Dam [32] made a fence height study with an NREL 5-MW blade of 63 m span. The fence height study was made at the same constant spanwise location or maximum chord location, at 13.7 m from the blade baseline. Figure 21.19 illustrates the percent change in power and thrust for different fence heights, for a free stream velocity of 11 m/s and rotor speed of 11.89RPM. It can be appreciated a nearly constant difference between power and thrust for large fence heights ($h_{fence} > 5\%c_{max}$) and the maximum power values for heights between 1 and $2.5\%c_{max}$. The thrust and power curves are very pronounced for small fence heights ($h_{fence} < 3\%c_{max}$). At the spanwise position of $2\%c_{max}$ is located the most favorable fence height, with a power increase of 0.67% and a thrust increase of 0.34% (See Fig. 21.19).

The previous study was made at the same constant spanwise location or maximum chord location; so now a fence location study is needed in order to determine the optimal place where it should be located. Fence locations from 9.2 through 15.7 m are studied in 0.5 m increments with a fence height of $10\%c_{max}$. The free

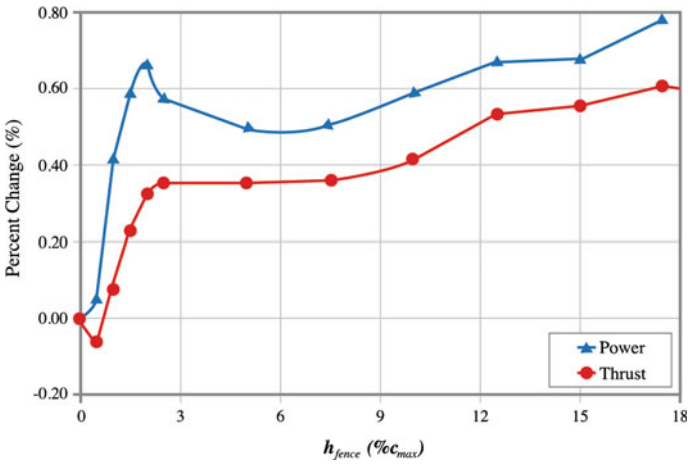

Fig. 21.19 Percent change in rotor power and thrust for different fence heights relative to the baseline NREL 5 MW blade (Chow and Van Dam [32])

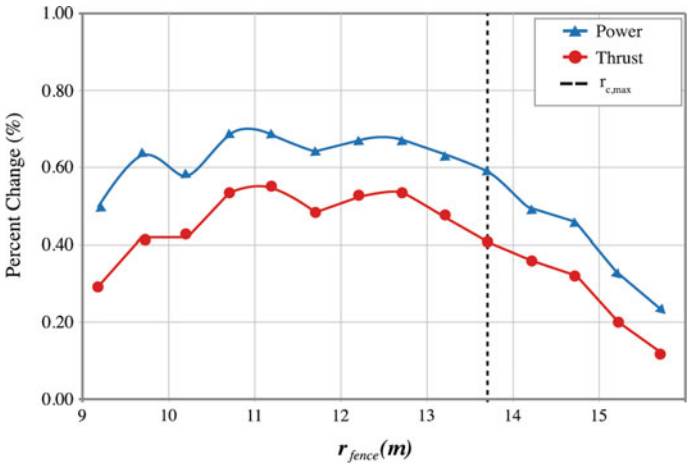

Fig. 21.20 Percent change in rotor power and thrust for various fences located at various spanwise fence locations relative to the baseline NREL 5 MW blade (Chow and Van Dam [32])

stream wind and rotor speeds remain constant as in the previous study (11 m/s and 11.89RPM, respectively). Figure 21.20 illustrates the thrust and power curves and their relation, almost constant over the entire range of spanwise locations studied, with a relatively larger increment in power capture of 0.15% in comparison to thrust. The effectiveness of the fences clearly gets worse when fences are located further and further outboard beyond maximum chord.

21.4.1.5 Spoilers

In general terms, the shape of a wind turbine blade can be defined in three regions (See Fig. 21.21)

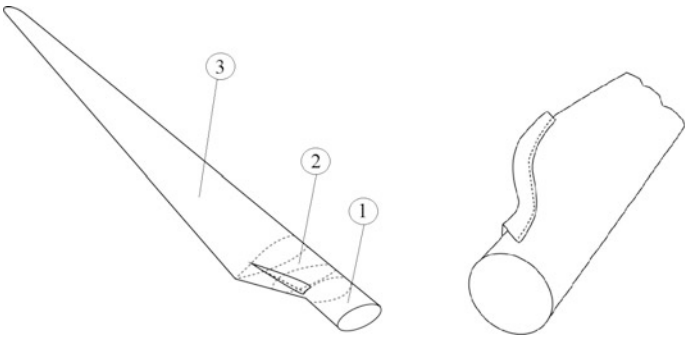

Fig. 21.21 Regions of a wind turbine blade with a spoiler device [33]

1. The nearest region to the hub (circular section).
2. The transition region between the circular section and the airfoil region.
3. The airfoil region.

The root and transition region, because of their section, do not help to the energy production of the wind turbine and even decreases it due to drag. These sections of wind turbines often work in stall situations, especially at high wind speeds. Therefore it is desirable a mechanism, such as spoilers [33], to increase the lift on these conditions (and not to stop) and for increasing the power generated by the turbine. The spoiler is assembled in the inboard part of the blade, i.e. the part nearest the hub, and particularly to the transition region of the blade, as shown in Fig. 21.22. A realistic estimate of the potential performance improvement is 1–1.5% of annual energy yield compared to conventional wind turbine blades without such spoilers. This provides a substantial economic benefit compared to the additional manufacturing costs related to the manufacturing of blades with such spoilers. However, this device presents a main disadvantage for its application in wind turbines against aerodynamics, the fact that the blades must work with higher angles of incidence.

21.4.2 Active Control Systems

21.4.2.1 Traditional Trailing-Edge Flaps

Before coming as a candidate for wind turbine control, traditional trailing-edge flaps were used previously with good results in aircraft load control. The National Renewable Energy Laboratory (NREL) began and carried out their investigations throughout the 1990s in order to improve wind turbines performance with this type of active control system.

The trailing-edge flaps vary the airfoil camber. The lift and the camber line, which is a measure of the amount of airfoil curvature, are directly related. The more curve the camber line is, the more lift the airfoil will generate. So, deploying the flap on the pressure side a lift increase is obtained and deploying it on the suction side a lift reduction is obtained.

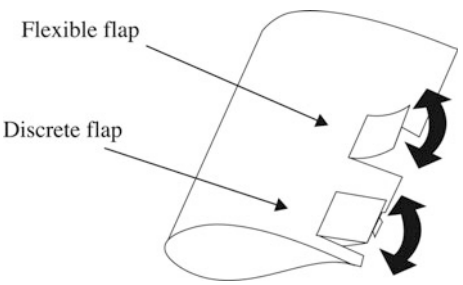

Fig. 21.22 Airfoil with discrete flap and flexible flap

They can be assembled in two ways: either as discrete flaps or flexible flaps (See Fig. 21.22).

1. *Discrete trailing-edge flap*: Conventionally used in aircraft, also known as ailerons are assembled in the blade (hinged) and require a moment over the hinge to achieve the required position. They provide good results in terms of power regulation and load alleviation. The development cost to integrate them in the blade should not be high considering all the background experience with this type of device in aviation.
2. *Flexible trailing-edge flap*: Their addition into the wind turbine blade is similar than discrete flaps. However, in this case there is no need for implementing rotating shafts mounted at the sides of the flaps. Therefore it is possible to produce the flexible flaps in modules which are attached to the blade only via a single connecting surface.

Its application in wind turbines presents some drawbacks, such as the size and weight that can reach the device and the mechanical actuators necessaries for its deployment. The aero-acoustic noise during operation and the energy required for deployment are some pending parameters to improve for its application.

21.4.2.2 Air Jet Vortex Generators

The air jet vortex generator (AJVG) was first suggested by Wallis et al. [34], where circular jets issuing from a surface (airfoil) were used to produce "persistent velocity" for the purpose of delaying turbulent separation. It was discovered that a normal jet issuing into the free stream would produce a pair weak counter-rotating vortices that would pass downstream. Wallis chose a cross-stream jet that was angled at a pitch angle of 45° to the airfoil surface. The vortex remains embedded in the boundary layer over the airfoil and entrains high-momentum air from the undisturbed flow into the boundary layer. This process helps mitigate boundary layer separation and leads to an increase in C_{Lmax} and angle of attack at stall α_{stall} (See Fig. 21.23).

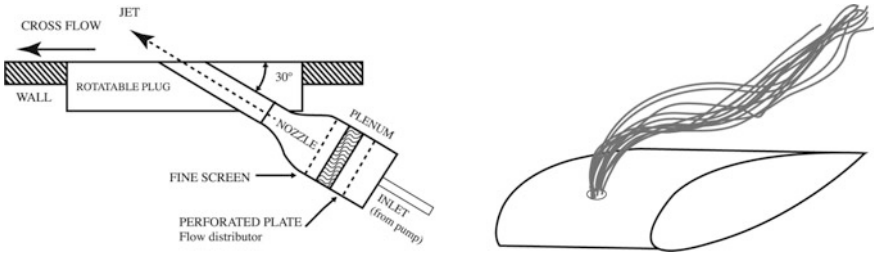

Fig. 21.23 Schematic of AJVG actuator with a pitch angle of 30° and streamlines representation in a wind turbine blade [3]

Johnston and Nishi [35], in 1990, studied more in detail the AJVG choosing a number of simple cases to assess the effects of the vortices. However, there was a problem in this study with the measurement system because the scale of the vortex compared to the size of the hole-probe (used to derive the vorticity in the cross-flow plane) and the sampling grid was quite small. Consequently, it was not possible to sample the vorticity in the region where the vortex was close to the wall, so too much information of the vortex was lost.

A study by Compton and Johnston [36] in 1992 showed that, even for the strongest case tested, the air-jet was qualitatively compared with the vortex produced from a VG but the dissipation of the vorticity takes place at a much greater rate for the AJVG.

Lately, investigations with pulsed vortex generator jets (PVGJ), which are placed in the leading edge, have been gaining interest because they are more effective in delaying stall due to two factors mainly:

1. The improved vorticity production related with the impulsively started jet flow.
2. The reduction in mass flow compared to steady jets due to the reduced duty cycle.

The AJVG presents some interesting characteristics for wind turbine applications. One of the most important is its wide controllability, which allows to modify the parameters of vortex generation according to the circumstances. Its location in the leading edge makes it easy to install, however, it requires the installation of compressed air lines and determine how much air would be necessary and its power expenditure. Other factor that must be taken into account is to maintain the exit ports free of outside influences (insects, dirt or ice).

21.4.2.3 Synthetic Jets

Initially investigated by James et al. [37] in 1996, this type of active flow control creates streamwise vortex similar to those created by PVGJ but with a significant difference, a synthetic jet adds momentum to airflow without adding mass. A conventional jet sucks in air, accelerates this air, and exhausts the air out of a different opening, maintaining airflow. In contrast, a synthetic jet alternates sucking in and blowing out air through the same opening at high frequencies. One method for creating this jet is to use a piezoelectric diaphragm to act as the oscillating membrane. When this membrane oscillates, it sends puffs of air through the cavity and out of a small surface hole. Figure 21.24 illustrates the operating principle of this type of active control device.

Pechlivanoglou [38] summarized the main characteristics of synthetic jets, their mechanical structure, integration, costs and reliability. They are usually located at 10–20% c (close to the leading edge) and can be installed at any angle to the aerodynamic surface. In this case there would not be any problem in terms of space to integrate the synthetic jets. Another factor to be taken into account about their

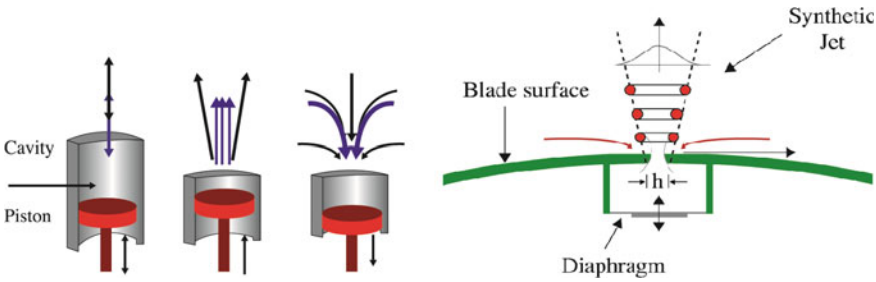

Fig. 21.24 Synthetic jet production principle

integration in wind turbine blades is the structural consequences of the surface discontinuities caused by the synthetic jet slots/holes. The most possible solution to mitigate this trouble would be the integration of additional parts in the blade structure and consequently, changing the laminate structure of the blade.

The existence of synthetic jet mechanisms inside the blade structure increases the complexity of the blade as well as the required maintenance effort. For this reason the flow control mechanisms (individual or integrated in inserted units) should be removable and replaceable in such a way that their maintenance and replacement is fast and cost effective.

Numerous investigations, experimental [39] and numerical [40] have supported the efficiency of this device in aerodynamics achieving significant maximum lift increases, about 29%, and delaying boundary layer separation.

21.5 Energy Efficiency of Active and Passive Flow Control Devices

The cost of electricity generated by wind turbines depends on the location of the wind farm, i.e. the number of full load hours per year. In low wind areas the costs ranges from 0.05 to 0.07 €/kWh and at windy coastal areas the costs ranges from 0.09 to 0.11 €/kWh [41]. A place at the highest point possible and away from obstructions (forests, towers, rocky outcrops) corresponds to the best location for a wind turbine, where the wind can concentrate and get higher speeds.

Currently, it is not easy to quantify in terms of profits the improvement of these flow control devices because it depends on many variables such as the size and weight of each wind turbine or the wind speed average over the year. In terms of lift enhancement, active control devices, in general, present better results than passive control devices, and therefore to improve the energy efficiency of wind turbines, even though they are more costly to integrate in the blades and to maintenance.

Pechlivanoglou [38], with his experimental investigations in large wind tunnel facilities testing different flow control devices, could check the advantages and

disadvantages that present each device in costs (development, integration, maintenance, operation) and therefore get some preliminary conclusions about the cost of energy and their efficiency.

21.6 Conclusion

The wind-power sector is growing rapidly and shows evidences that it will continue in that way in the following years. The growth of this industry becomes in an increase in the size of wind turbines, which leads to an increase in fatigue and structural loads that the system have to support. This may also lead to higher O&M costs to maintain the structure lifetime. The active and passive flow control devices are presented as a solution to these problems. Small size and lightweight are some of their main characteristics and can offset turbulent wind loads. Improvements in these types of devices can increase the life-cycle of wind turbines, power production, system performance and reduce the COE. This decrease in COE would allow to increase the competitiveness in price against traditional sources or other renewable alternatives. The purpose of this chapter was not to make a direct comparison between the different types of devices, reach a conclusion or make a recommendation to choose one device or another. The goal was just to present to the reader a review of today's research in this field that could make major contributions to improve wind turbine control in the next years.

Acknowledgements I would like to take the opportunity to thank Dr. Unai Fernandez Gamiz, from Nuclear Engineering and Fluid Mechanics Department of University of the Basque Country of Vitoria-Gasteiz, for his support for the performance of this chapter, and his willingness to share bibliography, time and knowledge. This work was supported by both the Government of the Basque Country and the University of the Basque Country UPV/EHU through the SAIOTEK (S-PE11UN112) and EHU12/26 research programs, respectively.

References

1. The European Wind Energy Association (EWEA) (2015) Wind in power: European statistics. http://www.ewea.org/fileadmin/files/library/publications/statistics/EWEA-Annual-Statistics-2014.pdf
2. The Global Wind Energy Council (GWEC) (2015) Global wind statistics 2015. http://www.gwec.net/wp-content/uploads/vip/GWEC-PRstats-2015_LR_corrected.pdf
3. Johnson SJ, Van Dam CP, Berg DE (2008) Active load control techniques for wind turbines. Sandia National Laboratories. http://windpower.sandia.gov/other/084809.pdf. doi:10.2172/943932
4. Committee on Assessment of Research Needs for Wind Turbine Rotor Materials Technology (1991) Assessment of research needs for wind turbine rotor materials technology. National Academy Press, Washington

5. Poore R, Lettenmaier T (2003) Alternative design study report: WindPACT advanced wind turbine drive train designs study. National Renewable Energy Laboratory. http://www.nrel.gov/docs/fy03osti/33196.pdf. doi:10.2172/15004456
6. Wood RM (2002) A discussion of aerodynamic control effectors (ACEs) for unmanned air vehicles (UAVs). Paper presented at AIAA's 1st technical conference and workshop on unmanned aerospace vehicle, systems, technologies and operations, Portsmouth, 20–23 May 2002. doi:10.2514/6.2002-3494
7. Corten GP (2007) Vortex blades, oral presentation, WindPower 2007, Los Angeles
8. Taylor HD (1947) The elimination of diffuser separation by vortex generators. United Aircraft Corporation Report No. R-4012-3
9. Fernandez-Gamiz U, Velte CM, Réthoré PE, Sørensen NN, Egusquiza E (2016) Testing of self-similarity and helical symmetry in vortex generator flow simulations. Wind Energy 19 (6):1043–1052. doi:10.1002/we.1882
10. Pearcey HH (1961) Introduction to shock induced separation and its prevention by design and boundary layer control. In: Lachmann GV (ed) Boundary layer and flow control. Its principles and applications, vol 2. Pergamon Press, Oxford, pp 1170–1355. doi:10.1016/B978-1-4832-1323-1.50021-X
11. Godard G, Stanislas M (2006) Control of a decelerated boundary layer. Part 1: optimization of passive vortex generators. Aerosp Sci Technol 10(3):181–191. doi:10.1016/j.ast.2005.11.007
12. Bender EE, Anderson BH, Yagle PJ (1999) Vortex generator modeling for Navier-Stokes codes. In: 3rd ASME/JSME joint fluids engineering conference, San Francisco, 18–23 July 1999
13. Jirásek A (2005) Vortex-generator model and its application to flow control. J Aircr 42 (6):1486–1491. doi:10.2514/1.12220
14. Fernandez-Gamiz U, Réthoré PE, Sørensen NN, Velte CM, Zahle F, Egusquiza E (2012) Comparison of four different models of vortex generators. In: Proceedings of EWEA 2012—European wind energy conference & exhibition. European Wind Energy Association (EWEA)
15. Velte CM, Okulov VL, Hansen MOL (2011) Alteration of helical vortex core without change in flow topology. Phys Fluids 23(5):051707. doi:10.1063/1.3592800
16. Zamorano-Rey G, Garro B, Fernandez-Gamiz U, Zulueta-Guerrero E (2015) A computational study of the variation of the incidence angle in a vortex generator. DYNA New Technol 2 (1):1–13. doi:10.6036/NT7357
17. Øye S (1995) The effect of vortex generators on the performance of the ELKRAFT 1000 kW turbine. In: 9th IEA symposium on aerodynamics of wind turbines, Stockholm
18. Miller GE (1984) Comparative performance tests on the Mod-2, 2.5-MW wind turbine with and without vortex generators. In: DOE/NASA workshop on horizontal axis wind turbine technology, Cleveland
19. Bak C, Bitsche R, Yde A, Kim T, Hansen MH, Zahle F, Gaunaa M, Blasques JPAA, Døssing M, Wedel H, Jens J, Behrens T (2012) Light rotor: the 10-MW reference wind turbine. In: Proceedings of EWEA 2012—European wind energy conference & exhibition. European wind energy association (EWEA)
20. Bak C, Zahle F, Bitsche R, Kim T, Yde A, Henriksen LC, Hansen MH, Blasques JPAA, Gaunaa M, Natarajan A (2013) The DTU 10-MW reference wind turbine, Danish Wind Power Research, Fredericia, 27 May 2013
21. Troldborg N, Zahle F, Sørensen N (2015) Simulation of a MW rotor equipped with vortex generators using CFD and an actuator shape model. In: 53rd AIAA aerospace sciences meeting, AIAA SciTech. doi:10.2514/6.2015-1035
22. Wilcox DC (2006) Turbulence modeling for CFD. DCW Industries, La Cañada
23. Menter FR (1993) Zonal two equation k-ω turbulence models for aerodynamic flows. AIAA J. paper 93-2906. doi:10.2514/6.1993-2906
24. Chow R, Van Dam CP (2006) Unsteady computational investigations of deploying load control microtabs. J Aircr 43(5):1458–1469. doi:10.2514/1.22562

25. Yen DT, Van Dam CP, Bräuchle F, Smith RL, Collins, SD (2000) Active load control and lift enhancement using MEM translational tabs. In: Proceedings of the fluids conference and exhibit, Denver, 19–22 June 2000. doi:10.2514/6.2000-2242
26. Tsai KC, Pan CT, Cooperman AM, Johnson SJ, Van Dam CP (2015) An innovative design of a microtab deployment mechanism for active aerodynamic load control. Energies 8(6):5885–5897. doi:10.3390/en8065885
27. Oerlemans S, Fisher M, Maeder T, Kögler K (2009) Reduction of wind turbine noise using optimized airfoils and trailing-edge serrations. AIAA J 47(6):1470–1481. doi:10.2514/1.38888
28. Stiesdal H, Enevoldsen PB (2003) Flexible serrated trailing edge for wind turbine rotor blade. European Patent Office, EP 1 314 885 B1, 28 May 2003
29. Howe M (1991) Noise produced by a sawtooth trailing edge. J Acoust Soc Am 90(1):482–487. doi:10.1121/1.401273
30. Oerlemans S, Schepers J, Guidati G, Wagner, S (2001) Experimental demonstration of wind turbine noise reduction through optimized airfoil shape and trailing-edge serrations. In: Proceedings of the European wind energy conference and exhibition, Copenhagen, 2–6 July 2001
31. Quell P, Petsche M (2009) Rotor blade for a wind power station. US Patent 7,585,157 B2, 8 Sept 2009
32. Chow R, Van Dam CP (2011) Inboard stall and separation mitigation techniques on wind turbine rotors. In: 49th AIAA aerospace sciences meeting including the new horizons forum and aerospace exposition, Orlando, 4–7 January 2011. doi:10.2514/6.2011-152
33. Lenz K, Fuglsang P (2008) Wind turbine having a spoiler with effective separation of airflow. European Patent Office, EP 2 141 358 A1, 12 Dec 2008
34. Wallis RA (1960) A preliminary note on a modified type of air jet for boundary layer control. Aeronautical Research Council, Current-Paper 513, London
35. Johnston J, Nishi M (1990) Vortex generator jets–a means for passive and active control of boundary layer separation. AIAA J 28(6):989–994. doi:10.2514/3.25155
36. Compton DA, Johnston JP (1992) Streamwise vortex production by pitched and skewed jets in a turbulent boundary layer. AIAA J 30(3):640–647. doi:10.2514/3.10967
37. James RD, Jacobs JW, Glezer A (1996) A round turbulent jet produced by an oscillating diaphragm. Phys Fluids 8(9):2484–2495. doi:10.1063/1.869040
38. Pechlivanoglou G (2013) Passive and active flow control solutions for wind turbine blades. Dissertation, Technische Universitat Berlin
39. Seifert A, Bachar T, Koss D, Shepshelovich M, Wygnanski I (1993) Oscillatory blowing: a tool to delay boundary-layer separation. AIAA J 31(11):2052–2060. doi:10.2514/3.49121
40. Donovan JF, Kral LD, Cary AW (1998) Active flow control applied to an airfoil. In: 36th AIAA aerospace sciences meeting and exhibit, Reno, Nevada. doi:10.2514/6.1998-210
41. Krohn S, Morthorst PE, Awerbuch S (2009) The economics of wind energy, a report by the European wind energy association. http://www.ewea.org/fileadmin/files/library/publications/reports/Economics_of_Wind_Energy.pdf